

Hollow-cone Spray of Viscous Liquid in High-pressure Gas Environment - Experimental Investigation for the Application of New Liquid Fuels to Gas-turbine -

T. SUZUKI*,

Dept. of Mech. Engng, Toyohashi University of Technology, JAPAN

H. NISHIDA, N. HASHIMOTO and Y. OZAWA

Energy Engng Research Lab., Central Research Institute of Power Industry, JAPAN

Abstract

Experimental investigations were performed on the hollow-cone spray of viscous liquids in high-pressure gas environment, aiming to obtain fundamental knowledge which was indispensable to survey the applicability of non-conventional new liquid fuels for the gas-turbine power-plant. Test liquid employed were water, diesel fuel, palm methyl ester (PME) and silicone-oil #10. The ambient gas was nitrogen of room temperature. The test nozzle was small-sized swirl atomizer; Delavan oil burner nozzle 60°A-0.85. The liquid flow-rate was ranging from 50 to 140cc/min, and the ambient-gas pressure was ranging from 0.1 to 1.0MPa. The behavior of injected liquid-sheet and ensuing spray-flow were observed in detail by flash photography. The apical-angle and the breakup-length of conical liquid-sheet and the cone-angle of spray were evaluated from the photographs. The Sauter mean diameter of spray was measured by the laser diffraction method, and the spray flow field was investigated by the PIV technique. The effects of liquid flow-rate, ambient-gas pressure and properties of test liquid upon the atomization characteristics were revealed. The spray contracted and showed bell-shape at high gas pressures. When viscous liquid was injected, the spray contraction was observed in wider range of flow-rate, and several peculiar atomization manners were also observed. The flow mechanisms were discussed in this study.

Introduction

Power plant of gas-turbine combined cycle (GTCC) has attracted attentions, because of its high power-generation efficiency and wide load-adjustment range [1]. Light oil and natural gas are mainly used for fueling the power plant nowadays. Considering from the standpoint of energy security, alternative energy resource should be looked for. Bio-liquid fuels and non-conventional fossil oils are the candidates for the alternative energy resource [2]. The problem is that most of these new fuels have higher viscosity. The liquid fuel is sprayed into compressed high-pressure air in the current gas-turbines. The pressure atomizers, especially the swirl atomizer of hollow-cone spray, have been widely used. Therefore, the spray characteristics of swirl atomizer in high-pressure gas environment have been studied by many researchers [3]. The new liquid fuels should also be supplied by means of atomizers. It is convenient that the swirl atomizer can be used to spray the fuels. To evaluate the applicability of these new liquid fuels to the gas-turbine power-plant, fundamental knowledge is indispensable on the hollow-cone spray of viscous-liquid in high-pressure gas environment.

In the present study, experimental investigations were performed on the hollow-cone spray of viscous liquids in high-pressure gas environment using the setup of small-sized swirl-atomizer installed in pressure vessel. Water spray test was performed first with changing the liquid flow-rate and the ambient-gas pressure. The breakup behavior of injected liquid-sheet and ensuing spray-flow were observed in detail by flash photography. The apical-angle and the breakup-length of conical liquid-sheet and the cone-angle of spray were evaluated from the photographs. The Sauter mean diameter of spray was measured by the laser diffraction method, and the spray flow field was investigated by the particle image velocimetry (PIV) technique. The effects of the liquid flow-rate and the ambient-gas pressure upon the atomization characteristics were examined. Although the spray spread into a form of clear hollow-cone at relatively low ambient-gas pressures, the spray contracted and showed bell-shape at higher ambient-gas pressures. The mechanism of spray contraction was discussed with presenting the model of spray flow field. The spray tests of diesel fuel and palm methyl ester (PME) were performed next. The spray of silicone-oil #10 was also investigated in the place of high-viscous liquid. The higher viscosity the liquid had, the longer cone of liquid-sheet was suspended at nozzle-exit. The spray contraction could be observed in wider range of the liquid flow-rate when liquid was viscous. However, the Sauter mean diameter of spray was not affected so much by the liquid-viscosity within this experimental range. When viscous liquid was injected, several peculiar atomization manners could be also observed; roll-up of smooth liquid-sheet, perforation of liquid-sheet and spray pulsation. The experimental range for each atomization manner was examined, and the mechanism of spray pulsation was discussed.

* Corresponding author: takashi@me.tut.ac.jp

Experimental Methods

Schematic illustration of experimental setup is shown in figure 1. The main body was a cylindrical pressure vessel of about 14ℓ with four observation windows on the side wall. On the central axis of the vessel, a small-sized swirl-atomizer nozzle was installed. Test liquid was pumped by plunger to the nozzle and injected downward as a conical liquid-sheet from the nozzle-exit. Four ventilating fans with mist filters were installed in the upper part of the vessel, to eliminate the fine particles which drifted and interfered with observation. In the lower part of the vessel, a honeycomb plate and a sheet of nonwoven were installed to prevent the spray splashing.

The behavior of injected liquid-sheet and ensuing spray-flow were observed in detail by flash photography. Aiming to obtain clear still image of liquid-sheet with high-speed motion, the backward illumination of Nd:YAG pulse laser (frequency-doubled) was used with the anti-speckle noise filter, NanoPhoton SK-11. The mean apical-angle, φ_{film} , of conical liquid-sheet and the mean breakup length, L_b , of liquid-sheet were evaluated from the photographs. By overlaying multiple images, the outside shape of spray was determined and the mean cone-angle, φ_{spray} , of spray was evaluated. The definitions of the mean breakup length, the mean apical-angle and the mean cone-angle were shown in figure 2. The liquid-sheet behavior was also observed using the high-speed video camera supplementary. The size of spray droplets was measured by the laser diffraction method [4]. The laser beam of 15mm diameter was located horizontally to penetrate the spray with crossing the centerline of spray at 50mm downstream from nozzle-exit. The size distribution and the Sauter mean diameter, D_{32} , of spray droplets within the laser beam were evaluated. The spray flow field was investigated by the particle image velocimetry (PIV) technique. The light-sheet of dual-pulse laser penetrated the spray along the vertical plane which included the centerline of spray, and the images of illuminated droplets were taken from the normal direction to the plane. Sequential two images were analyzed using Dantec FlowManager system, and the distribution of mean velocity of spray was obtained by averaging the results of 20 runs.

The test spray nozzle was Delavan oil burner nozzle 60°A-0.85, whose design capacity was 54cc/min at liquid injection pressure of 0.67MPa. The liquid flow-rate, Q_{liq} , was ranging from 50cc/min to 140cc/min, and the ambient-gas pressure, P_{amb} , was ranging from 0.1MPa to 1.0MPa. The ambient gas was nitrogen of room temperature. Test liquid employed were water, diesel fuel JIS#2, and palm methyl ester (PME) of Malaysia. Silicone-oil #10 was also employed in the place of high-viscous liquid. Physical properties of test liquids were listed in Table 1 [2]. Water has higher surface tension and lower kinematic viscosity than diesel fuel. PME has larger kinematic viscosity than diesel fuel. Silicone-oil #10 is more viscous than PME.

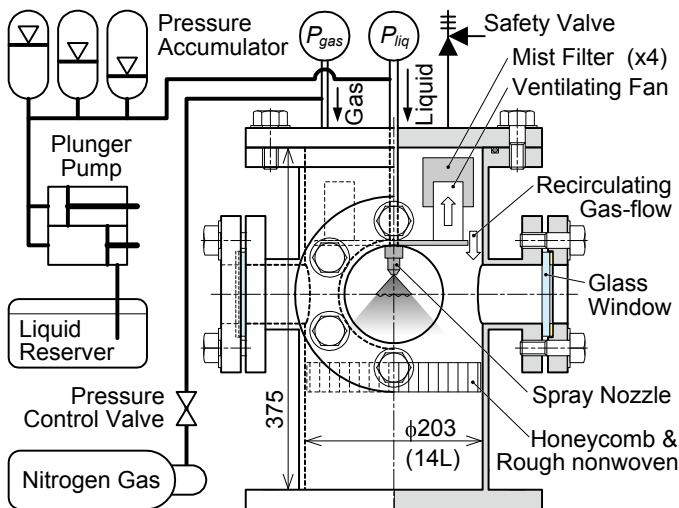


Figure 1 Schematic diagram of experimental setup.

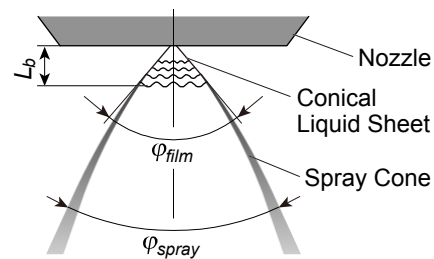


Figure 2 Definitions of mean breakup length of liquid-sheet, mean apical-angle of liquid-sheet and mean cone-angle of spray.

Table 1 Physical properties of test liquids. (Values in the parentheses indicate temperatures.)

Test Liquid	Density ρ_{liq} (kg/m ³)	Kinematic Viscosity ν_{liq} (mm ² /s)	Surface Tension σ (mN/m)
Water	995.65 (30°C)	0.801 (30°C)	72.28 (23°C)
Diesel Fuel JIS#2	825.2 (30°C)	3.29 (30°C)	28 (23°C)
Palm Methyl Ester (PME)	863.6 (30°C)	5.63 (30°C)	30.6 (23°C)
Silicone Oil #10	935 (25°C)	10.0 (25°C)	20.1 (25°C)

Results and Discussion

Water spray test

The spray of water was first investigated. Typical flash photographs of water spray are shown in figure 3(I). A conical liquid-sheet was injected from the nozzle-exit. The liquid-sheet fluctuated strongly and disintegrated into small droplets. The droplets spread to form a conical sheath of spray, and the hollow-cone spray was formed. When the liquid flow-rate, Q_{liq} , was relatively small and the ambient-gas pressure, P_{amb} , was relatively low, the liquid-sheet broke up at about 1mm downstream from nozzle-exit, as shown in (I)-(b) of the figure. At larger liquid flow-rate, the liquid sheet fluctuated stronger and broke up more rapidly, as shown in (I)-(a) of the figure. When the ambient-gas pressure was high, the spray-cone was less spread than that of low ambient-gas pressures, as shown in (I)-(d) of the figure. In other words, the spray contraction took place and the spray-cone became bell-shape. The spray contraction was remarkably observed in the range of relatively high ambient-gas pressures and relatively large liquid flow-rates, as was reported in the previous studies [3].

The spray-flow field was investigated by the PIV technique. Figure 4 shows typical velocity-vector diagrams indicating the mean velocity distributions of spray-flow on the vertical cross-section of spray. Each chart presents the velocity distribution in the half-side from where the light-sheet incidents. As shown in the figure, the spray-flow velocity was large in the zone of spray sheath. That is, the spray-sheath was shaped by the cloud of high-speed droplets. The velocity of spray-sheath decreased with flowing-down. A downward-flow was also detected along the centerline of spray. The downward-flow was not so first and the velocity did not change so much with downstream-distance. Images for PIV analysis (not shown in the manuscript) indicated that there were many fine droplets flowing downward in the core zone of spray. These fine droplets should flow into the core zone from the sheath zone. The surrounding gas should be drafted into the spray, as illustrated in figure 5. It was considered that the surrounding gas was entrained by the high-speed droplets of spray-sheath, because the velocity of spray-sheath decreased with flowing-down. As can be seen from (a)-(b) of figure 4, the velocity of spray-sheath was high when the liquid flow-rate was large. As can be seen from (b)-(d) of figure 4, the velocity of spray-sheath was smaller and decreased more rapidly with flowing-down when the ambient-gas pressure was higher. It can be also seen from figure 4(c)-(d) that the spray-sheath was deflected inward from its original straight-way when the ambient-gas pressure was high, corresponding to the spray contraction. The deflection should be due to the strong drafting gas flow of large density under high pressures.

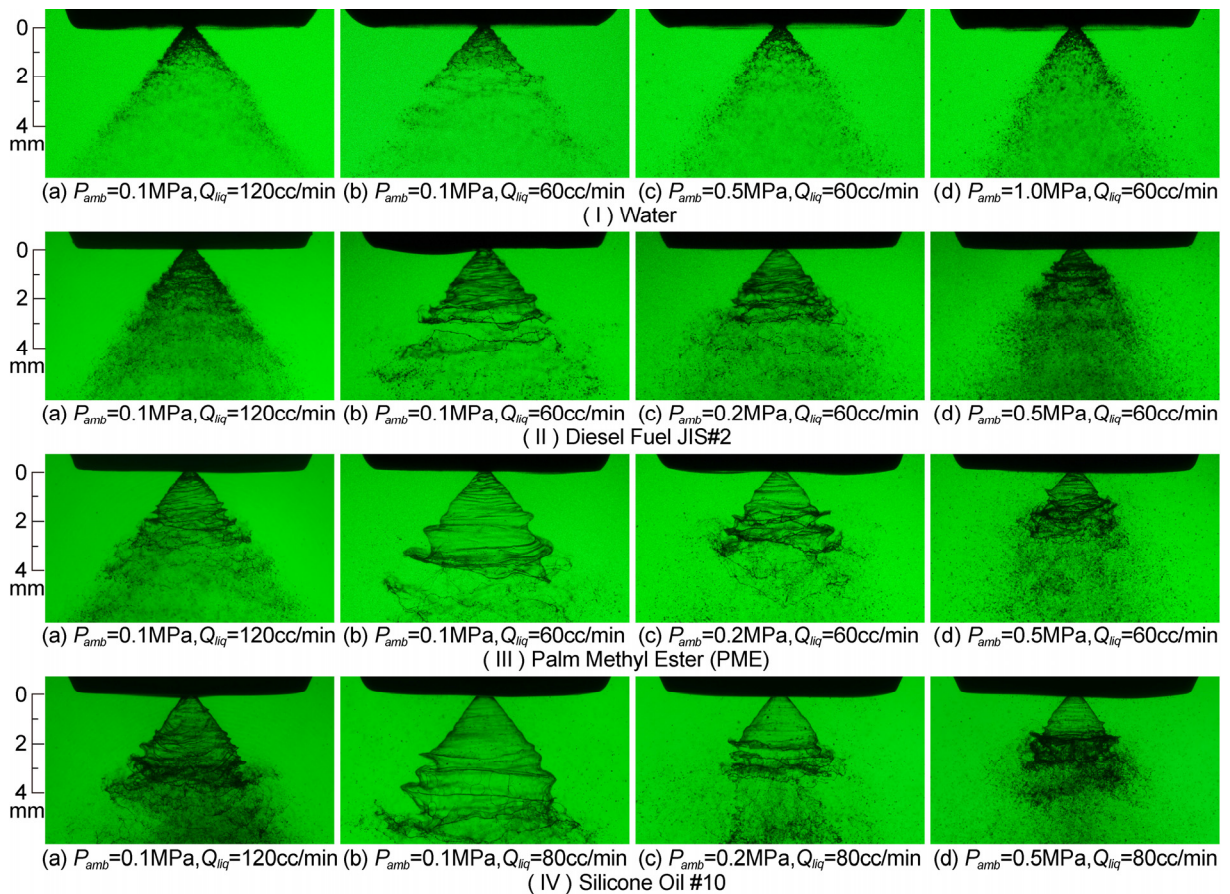


Figure 3 Typical flash photographs of liquid-sheet injected from small-sized swirl atomizer.

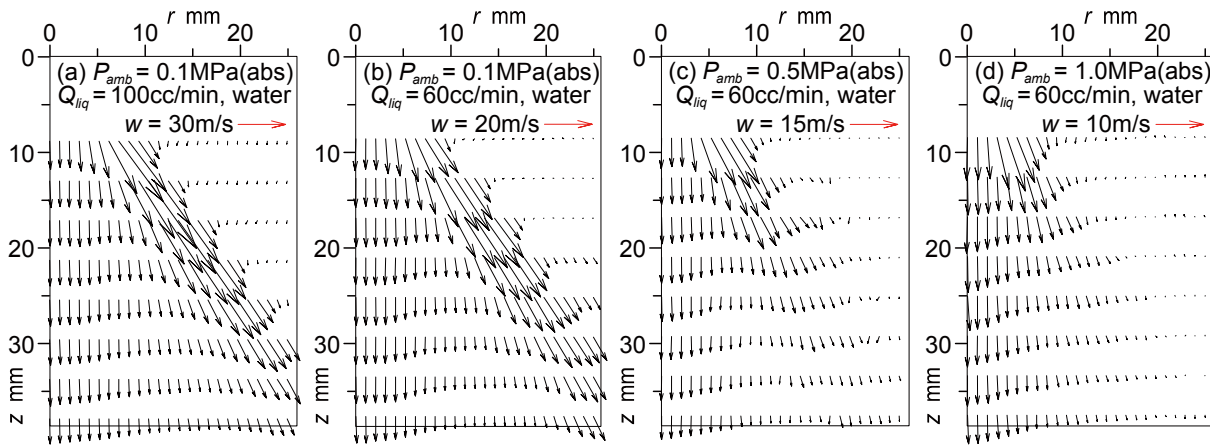


Figure 4 Typical velocity-vector diagram of spray on the vertical cross-section measured by PIV technique. (The red arrow in each chart indicates the vector size of standard velocity, w .)

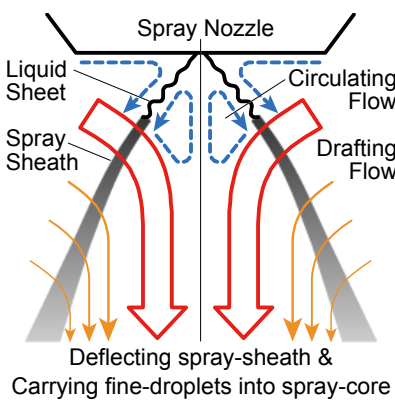


Figure 5 Model of spray flow field near nozzle exit showing drafting flow into spray-core.

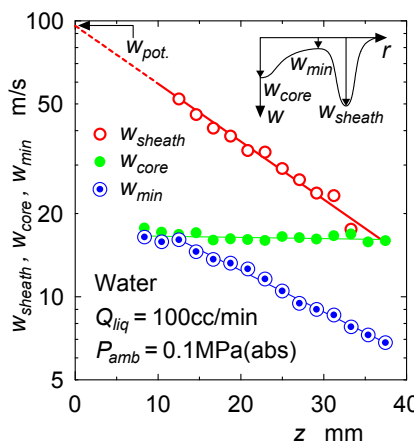


Figure 6 Variations of three representative velocities on the radial distribution of spray-velocity.

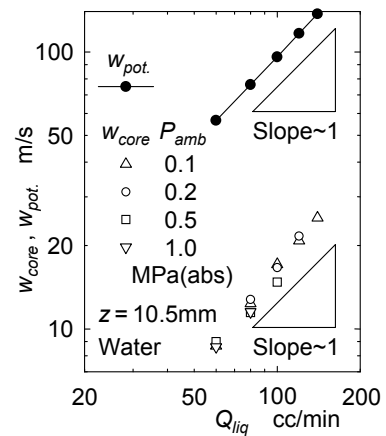


Figure 7 Variations of the spray-core velocity and the potential velocity of liquid-injection.

The radial distribution of spray velocity was examined. Figure 6 shows an example of stream-wise variations of three representative velocities on the radial distribution; the spray-sheath velocity, w_{sheath} , the spray-core velocity, w_{cores} , along the centerline, and the minimum velocity, w_{min} , inside spray-sheath. The definitions of these velocities are also shown in the figure. The spray-core velocity should correspond to the velocity of drafted gas-flow. The spray-sheath velocity and the minimum velocity decreased exponentially with downstream-distance, although the spray-core velocity did not change so much. The velocity at nozzle-exit, which was estimated by extrapolating the spray-sheath velocity variation to the nozzle-exit, almost agreed with the potential velocity, w_{pot} , of liquid injection estimated from the liquid-injection pressure. Figure 7 shows the variations of the spray-core velocity with increase of the liquid flow-rate for several ambient-gas pressure conditions. The spray-core velocity was evaluated at 10.5mm downstream from nozzle-exit. The variation of the potential velocity of liquid injection was also shown in the figure. The spray-core velocity did not change so much with the ambient-gas pressure. The spray-core velocity increased linearly with increase of the liquid flow-rate, and the slope of the spray-core velocity almost agreed with that of the potential velocity of liquid injection. These results supported that the velocity of drafted gas-flow did not change so much with downstream-distance, did not change so much with the ambient-gas pressure, and increased linearly with increase of the liquid flow-rate in proportion to the potential velocity of liquid injection.

Figure 8 shows the droplet size distributions of water spray measured by the laser diffraction method. The variations of the Sauter mean diameter, D_{32} , with increase of the liquid flow-rate are also shown in figure 9 for several ambient-gas pressure conditions. The Sauter mean diameter decreased with increase of the liquid flow-rate. The atomization should be promoted by the high liquid-injection velocity due to the large flow-rate. As can be seen from (d)-(f) of figure 8, the frequency of fine droplets, smaller than about $10\mu m$, became larger when the liquid flow-rate was large. The fine droplets should be selectively carried from the sheath zone into the core zone of spray by the drafted gas-flow, and the number density of fine droplets in the measuring volume became large. As also shown in figure 9, the Sauter mean diameter of high ambient-gas pressures was slightly larger than that of low ambient-gas pressures. The reason should be considered as follows: when the ambient-gas pressure was

higher, the liquid-sheet fluctuated stronger and broke up at the position closer to nozzle-exit. As the liquid sheet was thicker near nozzle-exit, larger droplets should be produced by the disintegration of liquid-sheet.

The characteristics of liquid-sheet and spray-flow were examined by analyzing the flash photographs. Figure 10(a) shows the variations of the mean breakup-length, L_b , of liquid-sheet with increase of the ambient-gas pressure for several liquid flow-rate conditions. The breakup-length decreased with increase of the ambient-gas pressure, as shown in the figure. The breakup-length also decreased with increase of the liquid flow-rate. By the high liquid-injection velocity due to the large liquid flow-rate, and by the large gas density due to the high ambient-gas pressure, the stronger fluctuation of liquid-sheet should be promoted. The stronger fluctuation should result in the rapid breakup of liquid-sheet near nozzle-exit.

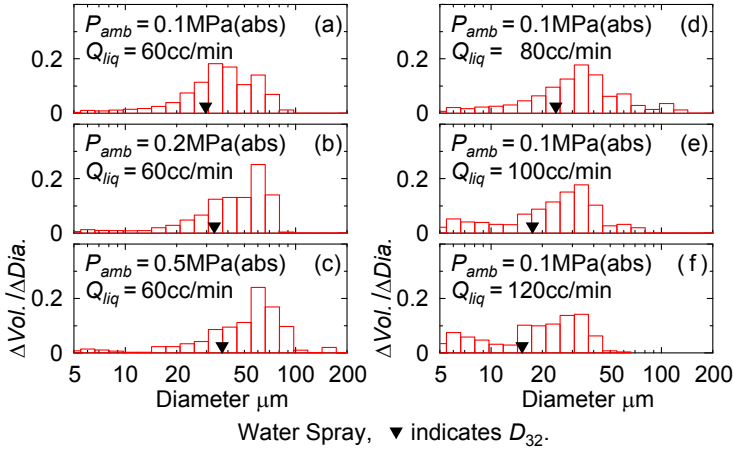


Figure 8 Typical examples of droplet size distributions of water spray measured by laser diffraction method.

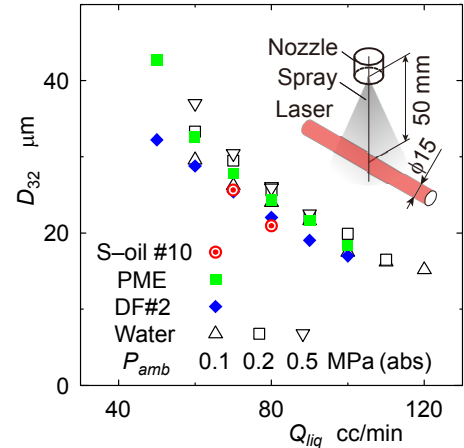


Figure 9 Variations of Sauter mean Diameter for each test liquid.

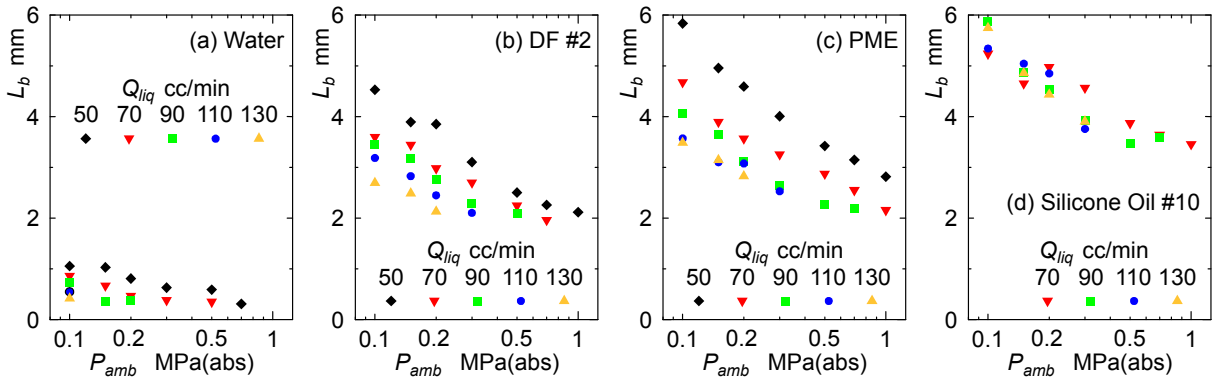


Figure 10 Variations of mean breakup length of liquid sheet with increase of ambient-gas pressure for several liquid-flow conditions.

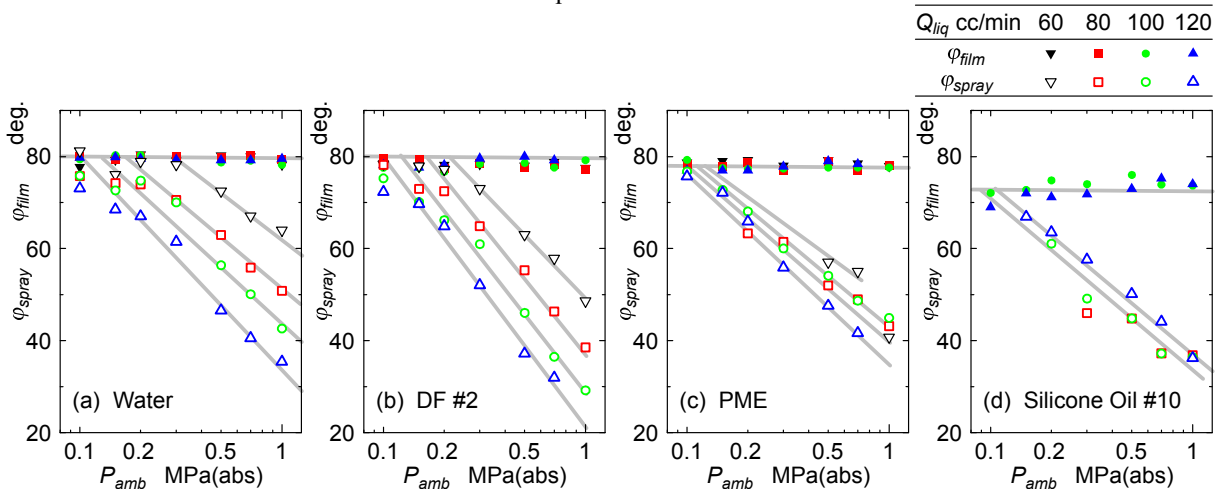


Figure 11 Variations of mean apical-angle of conical liquid-sheet and mean cone-angle of spray with increase of ambient-gas pressure for several liquid-flow conditions.

Figure 11(a) shows the variations of the mean apical-angle, φ_{film} , of conical liquid-sheet and the variations of the mean cone-angle, φ_{spray} , of spray with increase of the ambient-gas pressure for several liquid flow-rate conditions. The apical-angle of liquid-sheet was almost constant, about 80° , and was not affected by the ambient-gas pressure and the liquid flow-rate, as shown in the figure. However, the cone-angle of spray depended upon the experimental condition. In the case of the liquid flow-rate of 60cc/min, the spray cone-angle was almost equal to the apical-angle of conical liquid-sheet at low ambient-gas pressures, but the spray cone-angle started to decrease at about 0.3MPa of ambient-gas pressure and decreased exponentially with increase of the ambient-gas pressure. When the liquid flow-rate was larger, the spray cone-angle started to decrease at lower ambient-gas pressures. The decrease of the spray cone-angle should be the result of the spray contraction. The spray contraction was obvious when the ambient-gas pressure was high and the liquid flow-rate was large.

Spray tests of other liquids

The spray tests of diesel fuel and palm methyl ester (PME) were performed next. The spray of silicone-oil #10 was also investigated in the place of high-viscous liquid. The results of the photographic observations were shown in (II)-(IV) of figure 3. When diesel fuel was sprayed, a conical liquid-sheet was injected from nozzle-exit and the liquid-sheet fluctuated strongly and disintegrated into hollow-cone spray, as was observed in water spray. The liquid-sheet extended longer cone than that of water, as shown in figure 3(II). When PME was injected, cone of liquid-sheet was longer than that of diesel fuel, as shown in figure 3(III). The fluctuation of PME liquid-sheet was somewhat calmer than that of diesel fuel. When silicone-oil #10 was injected, rather large cone of liquid-sheet was observed. Several peculiar breakup manners were also observed, which will be discussed later. The spray of every test liquid showed the contraction manner when the ambient-gas pressure was high.

The variations of the Sauter mean diameter for each test liquid are shown in figure 9. In every case of test liquid, the Sauter mean diameter decreased with increase of the liquid flow-rate, as was observed in water spray. The Sauter mean diameter of diesel fuel spray was slightly smaller than that of water spray. This should be caused by the lower surface tension of diesel fuel than water. The Sauter mean diameter of PME spray was slightly larger than that of diesel fuel spray. Unexpectedly, the Sauter mean diameter of silicone-oil #10 spray was slightly smaller than that of PME spray. The reason could be considered as follows: The liquid-sheet of viscous liquid extended into longer cone, and the liquid-sheet became thinner during the long travel. Consequently the liquid-sheet should disintegrate into smaller droplets. The large viscosity of liquid would also prevent the secondary breakup of relatively large droplets and lumps produced by the primary breakup. These two mechanisms would cancel each other, and the liquid viscosity did not affect so much the Sauter mean diameter of spray within this experimental range.

Figure 10(b)-(d) respectively shows the variations of the mean breakup-length of liquid-sheet for each test liquid. In every case of test liquid, the breakup-length decreased with increase of the ambient-gas pressure and with increase of the liquid flow-rate, as was observed in water spray. The breakup-length of diesel fuel was larger than that of water, and the breakup-length of PME was larger than that of diesel fuel. The breakup-length of silicone-oil #10 was almost twice as long as diesel fuel. That is, the higher viscosity the liquid had, the longer the breakup-length became. It is considered that high viscosity of liquid prevented the breakup of liquid-sheet.

The variations of the mean apical-angle of conical liquid-sheet and the variations of the mean cone-angle of spray for each test liquid are shown respectively in figure 11(b)-(d). In every case of test liquid, the apical-angle was almost constant, as was observed in water spray. The liquid sheets of diesel fuel and PME had similar apical-angle, about 80° , to that of water. However, the apical-angle of silicone-oil #10 liquid-sheet was slightly smaller than that of other test liquids. The large viscosity of silicone-oil #10 should dump the swirling-flow in the nozzle, as was investigated in the previous study [5], and consequently the liquid circumvolution at nozzle-exit should become slower. In every case of test liquids, the spray cone-angle decreased with increase of the ambient-gas pressure. The spray cone-angle of diesel fuel also depended upon liquid flow-rate, as was observed in water spray. The larger the liquid flow-rate was, the smaller the spray cone-angle became. However, the spray cone-angle of PME did not depend upon the liquid flow-rate so much. The spray cone-angle of silicone oil #10 did not depend on the liquid flow-rate, either. At this stage, it was not clear why the degree of spray contraction did not depend upon the liquid flow-rate in case of viscous liquid.

When viscous liquid was injected, several peculiar atomization manners, as well as conventional atomization manner, could be observed. Flash photographs of the peculiar atomization manners are shown in figure 12. In some case, the liquid-sheet extended into large smooth-cone and the open-end rolled up abruptly, as shown in figure 12(a). In some case, the extended liquid-sheet was perforated before breakup, as shown in figure 12(b). In some case, the liquid-sheet disintegrated intermittently to form droplet clusters and the spray flow pulsated, as shown in figure 12(c). The experimental range for each peculiar manner was investigated. The results are shown in figure 13. When silicone-oil #10 was injected, each peculiar atomization manner could be observed in wide range of liquid flow-rate and ambient-gas pressure. However, the spray of PME showed each manner only in restricted range, as shown in figure 13. The spray of diesel fuel never showed these peculiar manners.

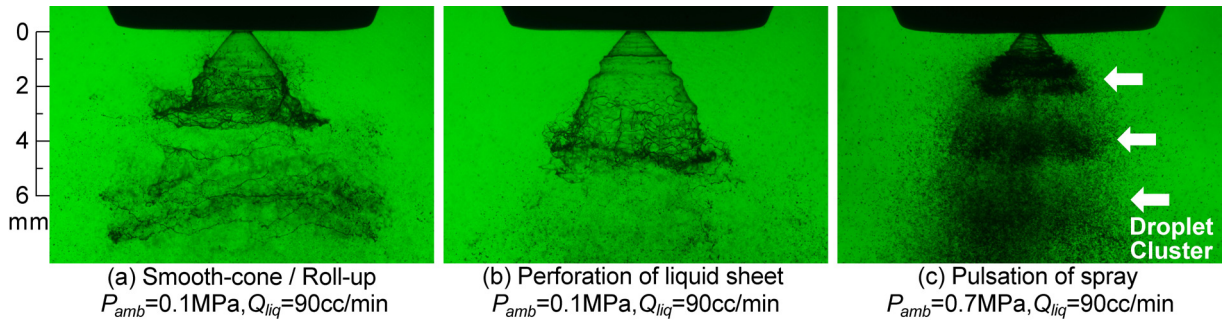


Figure 12 Flash photographs showing peculiar atomization manners of viscous liquid. (Silicone oil #10)

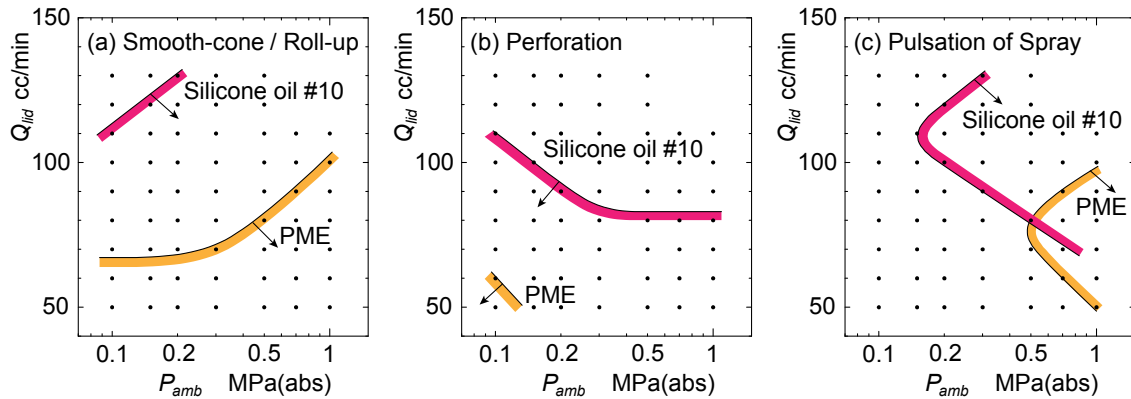


Figure 13 Observed ranges of peculiar atomization manners shown in figure 12. (Dots in each chart indicate experimental conditions of observation.)

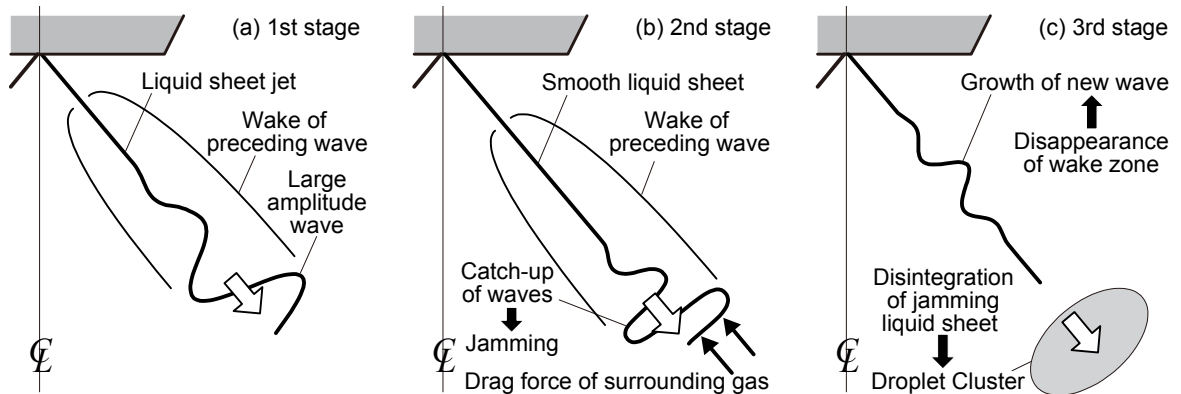


Figure 14 Model of spray pulsation mechanism.

The manner of the spray pulsation should be noteworthy, because it might be a cause of combustion oscillation if the swirl atomizer was used for spraying viscous-fuel in the power plant. Based on the detailed observation, the mechanism of the spray pulsation could be considered as follows: The liquid-sheet of viscous liquid was not easily broke up and extended to be a longer cone, and the fluctuation of liquid-sheet would grow into large amplitude wave, as shown in figure 14(a). As the upstream part of liquid-sheet should be in the wake zone of wavy liquid-sheet, the liquid sheet would not be exposed to the relative motion with surrounding gas, and the liquid-sheet would hardly fluctuate. Because the drag force of surrounding gas should act on the front-face of wavy liquid-sheet, the wavy liquid-sheet would decelerate, and the subsequent waves of liquid sheet would catch up to the preceding wave, as shown in figure 14(b). The jam of liquid sheet wave would occur in the leading part. Finally, the leading part would disintegrate to be droplet cluster, as shown in figure 14(c). As the wake of preceding wave disappeared, the liquid-sheet would start to fluctuate in the upstream, and it should return to the 1st stage. Similar breakup manner was observed during the experimental investigation of the radial liquid-sheet formed by the impingement of two liquid jets when liquid had high viscosity [6].

The data obtained in this study will be of use to survey the applicability of the non-conventional new liquid fuels with large-viscosity to the gas-turbine power-plant.

Summary and Conclusions

Using the setup of small-sized swirl-atomizer nozzle installed in pressure vessel, the experimental investigations were performed on the hollow-cone spray of viscous liquids in high-pressure gas environment. The behavior of injected conical liquid-sheet and ensuing spray-flow were observed in detail. The effects of liquid flow-rate, ambient-gas pressure and properties of test liquid upon the atomization characteristics were investigated.

- 1) The liquid-sheet fluctuated strongly and disintegrated to form a hollow-cone spray. The spray contracted and showed bell-shape at higher ambient-gas pressures. The spray contraction could be observed in wider range of liquid flow-rate when liquid was viscous. The mechanism of spray contraction was discussed.
- 2) The breakup-length of liquid-sheet decreased with increase of the ambient-gas pressure. The breakup-length also decreased with increase of the liquid flow-rate. The higher viscosity the liquid had, the longer the breakup-length became.
- 3) The spray cone-angle decreased with increase of the ambient-gas pressure, although the apical-angle of liquid-sheet was almost constant. The spray cone-angle of non-viscous liquid became smaller with increase of the liquid flow-rate, but the spray cone-angle of viscous liquid did not depend so much upon the liquid flow-rate.
- 4) The Sauter mean diameter of spray decreased with increase of the liquid flow-rate. The Sauter mean diameter increased slightly with increase of the ambient-gas pressure. However, the Sauter mean diameter was not affected so much by the liquid-viscosity within this experimental range.
- 5) The surrounding gas should be drafted into the spray core. It was found that the velocity of drafted gas-flow did not change so much with downstream-distance, did not change so much with the ambient-gas pressure, and increased linearly with increase of the liquid flow-rate.
- 6) When the viscosity of liquid was high, several peculiar atomization manners were also observed; roll-up of smooth liquid-sheet, perforation of liquid-sheet and spray pulsation. The experimental range for each atomization manner was examined, and the mechanism of spray pulsation was discussed.

Acknowledgements

Several students assisted with the experimental part of this work. The authors would like to express special thanks to Mr. Ryo Fukushima and Mr. Naoto Tezuka.

References

- [1] Meherwan, P.B., *Gas Turbine Engineering Handbook*, 4th ed., Butterworth-Heinemann, 2012.
- [2] Nishida, N. et al., *Energy Engineering Research Laboratory Rep.*, No.M07012 (2007). (in Japanese)
- [3] Lefebvre, A.H., *Atomizations and Sprays*, 204-222, Taylor&Francis, 1989.
- [4] Suzuki, T. et al., *Journal of ILASS-Japan*, 16-54: 34-46 (2007). (in Japanese)
- [5] Bayvel, L. and Orzechowski, Z., *Liquid atomization*, 252-280, Taylor&Francis, 1993.
- [6] Suzuki, T. et al., *Proc. of 20th Symposium on atomization (ILASS-Japan)*, 215-218 (2011). (in Japanese)